Load bearing capacity of prestressed concrete hollow core slabs taking into account tensile membrane action

Thomas Thienpont[1,*], Wouter De Corte[1], Robby Caspeele[1], Ruben Van Coile[1]

1. Department of Structural Engineering and Building Materials, Ghent University, Ghent, Belgium

[*]Corresponding author email: Thomas.Thienpont@UGent.be

Abstract

Tensile membrane action can considerably enhance the load-carrying capacity of longitudinally restrained concrete slabs. This additional capacity could delay, or even prevent, a structural collapse, and is therefore considered an important mechanism for increasing the robustness of concrete structures. Unlike reinforced concrete members, this beneficial effect is rarely considered in case of prestressed elements, such as precast hollow core slabs. Consequently, the reserve capacity of these commonly used floor elements due to tensile membrane action is a relevant topic for further investigations. Therefore, this paper investigates the beneficial effects of tensile membrane action in axially restrained prestressed concrete hollow core slabs. To this end, a detailed finite element model is developed in Abaqus. Numerical 4-point bending tests are performed to obtain the cracking patterns, displacements and failure loads. Subsequently, a brief parametric study is conducted to investigate the influence of the ultimate failure strain of prestressing steel on the ultimate load-carrying capacity of axially restrained concrete hollow core slabs taking into account tensile membrane action. The results indicate that tensile membrane action can, to some extent, enhance the load-carrying capacity of prestressed concrete hollow core slabs. However, the additional capacity that can be achieved strongly depends on the boundary conditions and the depth of the member.

Keywords: *Tensile membrane action, Hollow Core slab, Nonlinear analysis, Robustness.*

1. Introduction

1.1. Membrane action in reinforced concrete beams

When a longitudinally restrained concrete slab or beam is excessively loaded, or when a certain support is lost due to an accidental situation, membrane forces can be activated in order to establish a load transfer to the remaining supports. These membrane forces can considerably enhance the slab's load-carrying capacity, compared to predictions obtained from small deformation theories (Gouverneur, Caspeele, & Taerwe, 2013). In literature, the development of membrane forces is usually divided into two distinct categories: compressive membrane action (CMA) and tensile membrane action (TMA). In the former, compressive arching forces develop inside the slab as a result of the hindered outward displacement of the slab edges, which is prevented, to some degree, by the lateral stiffness of the surrounding structure (Brotchie & Holley, 1971; Muthu, Amarnath, Ibrahim, & Mattarneh, 2007). The CMA stage typically takes place up to a deflection approximately equal to the member's height; thereafter the compressive arches become unstable. If deflections increase even further, the TMA stage can develop, as illustrated in Figure 1. At this stage, the reinforcement starts acting as a catenary, which enables additional load bearing capacity under increasing deflections (Vecchio & Tang, 1990). Over the years, both types of membrane action have been studied extensively, and are shown to provide a significant beneficial contribution to the loading capacity and robustness of concrete structures in accidental load situations.

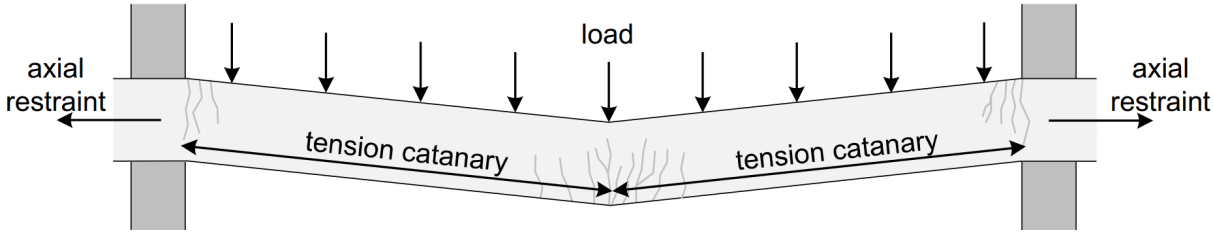

Figure 1: basic principle of tensile membrane action

1.2. Membrane action in prestressed concrete hollow core slabs

In recent decades, precast concrete hollow core (HC) slabs have become one of the most frequently used floor products on the construction market, due to their efficient design, economic production process and quick installation. Unlike reinforced concrete slabs and beams, the beneficial effects of membrane action on precast HC slabs have rarely been studied. In a previous study by the authors (Thienpont, Caspeele, & De Corte, 2020), the beneficial effect of CMA on the load bearing capacity of axially restrained prestressed concrete HC slabs was demonstrated. Herein the span-to-depth ratio, the concrete compressive strength and void dimensions were identified to have the largest influence on the ultimate capacity. In general, it was found that, for shorter spans, CMA could lead to a significant enhancement of the load bearing capacity, up to two times the capacity of the unrestrained member. However, the additional capacity of HC slabs due to TMA remains largely unknown. Therefore, the purpose of this paper is to quantify the additional capacity of precast HC slabs that can be obtained as a result of TMA. To this extent, numerical simulations are performed, and the influence of the restraint stiffness of the surrounding structure on the formation of TMA is studied.

2. Numerical model

2.1. Test setup and boundary conditions

To evaluate the development of TMA in axially restrained prestressed concrete HC slabs, a detailed 3D finite element model was developed in Abaqus (Dassault Systemes, 2014). Herein, a 4-point bending test setup with longitudinal end restraints was developed as presented in Figure 2. The restraints represent, in a simplified way, the horizontal stiffness of a surrounding structure.

As the purpose of this research is to solely study the development of TMA, the slab ends are free to expand and only the inward movement of the slab ends is restrained. This restraint configuration is based on an experimental test setup by Gouverneur (2014), which was used to demonstrate the additional capacity of reinforced concrete slabs due to TMA. Therefore, the configuration also allows for a direct comparison of the numerically obtained crack pattern with the cracks observed in the experiments on reinforced concrete slabs.

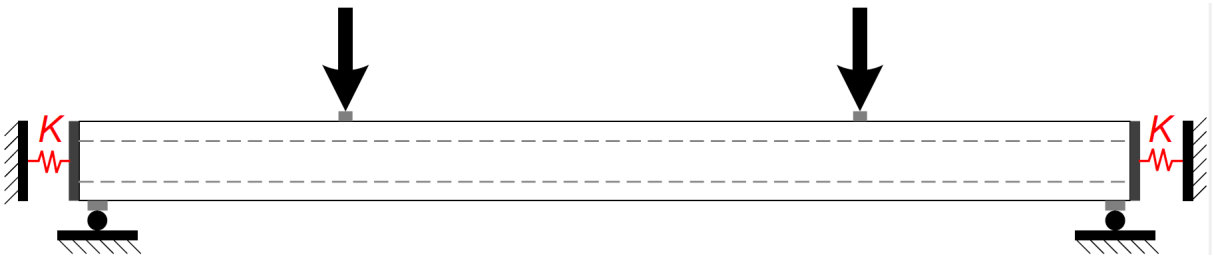

Figure 2: 4-point bending test setup, longitudinally restrained by two non-linear springs

The restraint configuration is numerically modelled using two non-linear spring elements, which produce a tensile force when the slab end moves inwards, but no compression force when the slab end moves outwards. This behaviour is schematically presented in Figure 3. Herein, the stiffness of spring elements in tension is characterized by the spring constant K_{spring}.

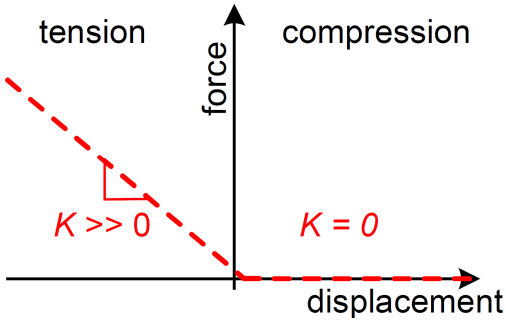

Figure 3: Schematic representation of a spring element, which only produces a force when being stretched

2.2. Hollow core sections

In this study, two HC sections are considered, as depicted in Figure 4. The 150 mm tall section geometry was obtained from a local Belgian precast manufacturer. The 200 mm tall section is based on a report by Walraven & Merckx (1983). Hereafter, these section will be referred to as HC150 and HC200. Details on the section geometry, the material properties and the level of prestressing are provided in Table 1.

The numerical calculation procedure consists of three steps. First, the prestressing force is numerically applied to the concrete section using the predefined field option in Abaqus. Next, the prestress is released, which causes shortening and upwards bending. Lastly, two line loads are applied at equal distances (i.e. ¼ of the span length) from the supports. By increasing these line loads, the deformations, the cracking patterns, membrane forces and ultimate capacities can be studied.

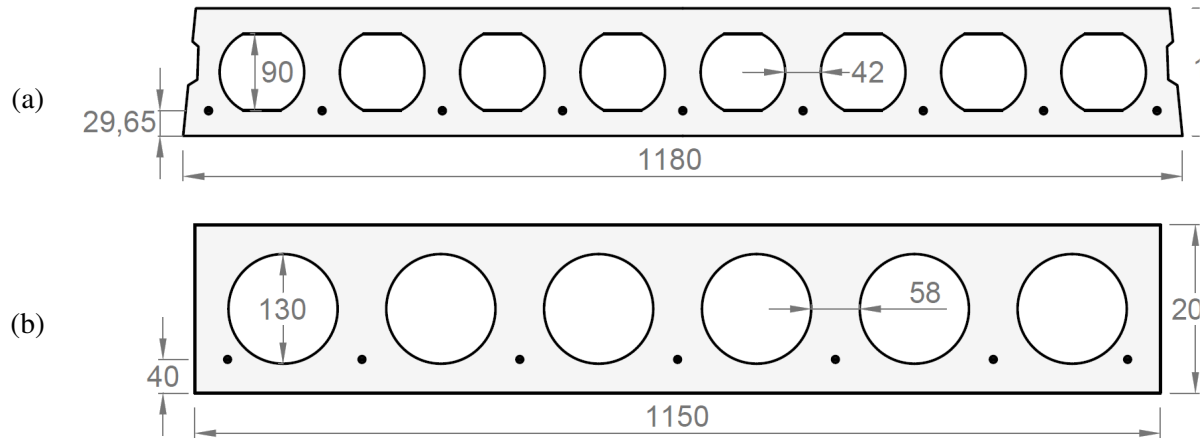

Figure 4: Hollow core slab sections; a) HC150; b) HC200 (Walraven & Mercx, 1983)

Table 1. Hollow core slab section geometries and material properties.

Section	h (mm)	b_w (mm)	A_c (cm²)	I_y (cm⁴)	f_c (MPa)	f_{pu} (MPa)	A_p (mm²)	f_{pi} (MPa)
HC150	150	350	1145	29465	50	1860	468	1116
HC200	200	370	1570	71050	50	1860	364	1240

2.3. Material models

The development of TMA in concrete members is characterized by large deformations and severe cracking. In order to model the behaviour of the concrete and prestressing steel in an adequate manner, non-linear material models were used. The concrete was modelled using the Abaqus concrete damaged plasticity model. Herein, the stress-strain diagrams for concrete in compression and tension were based on respectively EN 1992-1-2 (CEN, 2004b) and *fib* Model Code 2010 (Comité Euro- International du Béton, 2010). Figure 5.a and b depict the stress-strain relations in for concrete in compression and in

tension, for concrete with a compressive strength f_c = 50 MPa. As shown in Figure 5.c, after reaching the ultimate tensile strength f_{ct}, the concrete behaviour is modelled using a multilinear softening curve. The area under the softening curve corresponds to the tensile fracture energy. A multilinear curve was adopted, instead of the bilinear relationship proposed in *fib* Model Code 2010, to enhance the numerical stability of the model.

The tensile behaviour of prestressing steel is modelled using an idealized bilinear stress strain relation as suggested in EN 1992-1-1 (CEN, 2004a). This relation is determined by four parameters: the proof stress $f_{p0.1}$, tensile strength f_{pu} , modulus of elasticity E_p and ultimate strain ε_u. Figure 5.d depicts the stress strain diagram for a prestressing steel with tensile strength f_{pu} = 1860 MPa. After reaching the ultimate strain ε_u, the curve quickly drops to 100 MPa, to simulate a strand failure while remaining numerically stable.

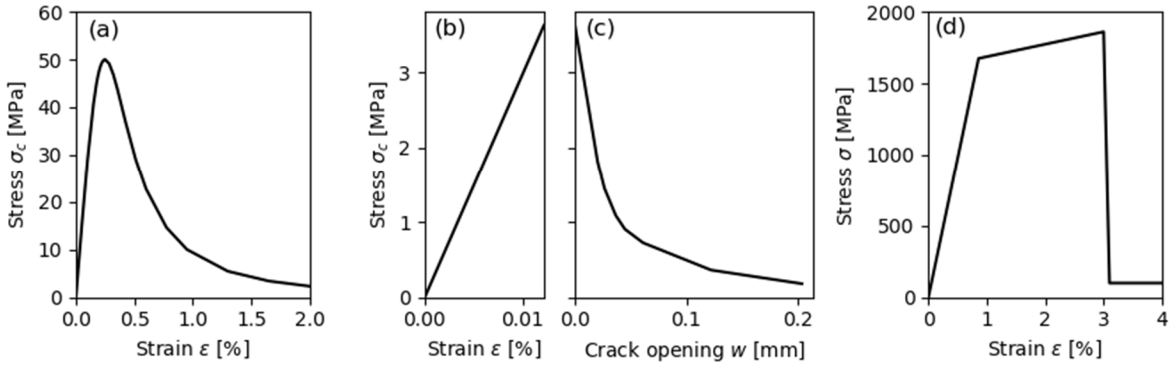

Figure 5: Material models: a) concrete compression stress-strain diagram; b) concrete tension stress-strain diagram; c) concrete tension softening stress vs crack opening diagram; d) steel stress-strain diagram

3. Results

3.1. Tensile membrane action in HC slabs

To study the development of TMA in precast HC slabs, the numerical model is employed to simulate displacement-controlled 4-point bending tests on axially restrained HC150 and HC200 sections. In all simulations, the material properties for concrete and steel are as presented in Table 1, and the ultimate tensile strain of the prestressing strands ε_u = 0.05.

In the following figures, the stiffness of the surrounding structure which prevents the inward movement of the slab ends is expressed in terms of the relative stiffness *k*. This parameter *k* relates the stiffness of the linear spring K_{spring} to the stiffness of the HC member $K_{HC\ slab}$, see Eq. (1). The stiffness $K_{HC\ slab}$ is calculated using Eq. (2).

$$k = \frac{K_{Spring}}{K_{HC\ slab}} \tag{1}$$

$$K_{HC\ slab} = \frac{E_c \cdot A_c}{l} \tag{2}$$

Herein, E_c is the modules of elasticity of the concrete, A_c is the cross-sectional area of the HC member and *l* is the length of the HC slab.

Figure 6.a depicts the calculated load-deflection curves of HC150 members with a free span of 6 m, for a wide range of relative restraint stiffnesses *k*, as well as the slab capacity in the unrestrained case. The curves in this figure coincide up to the point where the inward movement of the slab triggers the development of TMA. Thereafter, a significant increase of the load–displacement curves is observed. The slope of the curves strongly depends on the axial restraint stiffness. From the graphs, it is clear that a significant additional load bearing capacity can develop due to the (partially) restrained inward

movement of the slab ends. Even for a relatively small restraint stiffness $k = 0.025$, an additional capacity of more than 30% is reached. Figure 7.a provides an overview of the development of the horizontal catenary forces F_M in function of the vertical deflection. The catenary forces start to develop after a deflection of approximately 65 mm. The graph shows that the rate at which these TMA forces develop, as well as the maximum catenary force reached, increases with increasing restraint stiffness k.

Figure 6.b depicts the load-deflection curves from the HC200 members with a free span of 8 m. Here the additional capacity which can be achieved due to TMA is rather limited. Even in the highly restrained case where $k = 0.5$, the reserve capacity barely reaches 20%. From the above, it can be concluded that thicker HC slab sections have only a limited ability to develop catenary action, compared to more shallow sections. This result is in line with the experimental tests on axially restrained reinforced concrete slab strips by Guice & Rhomberg (1988). Herein, relatively higher TMA capacities were observed in thin slabs compared to thicker slabs. The development of the horizontal catenary forces in function of the vertical deflection is illustrated in Figure 7.b. Note that the catenary forces in this graph are also significantly smaller compared to the curves for the HC150 section.

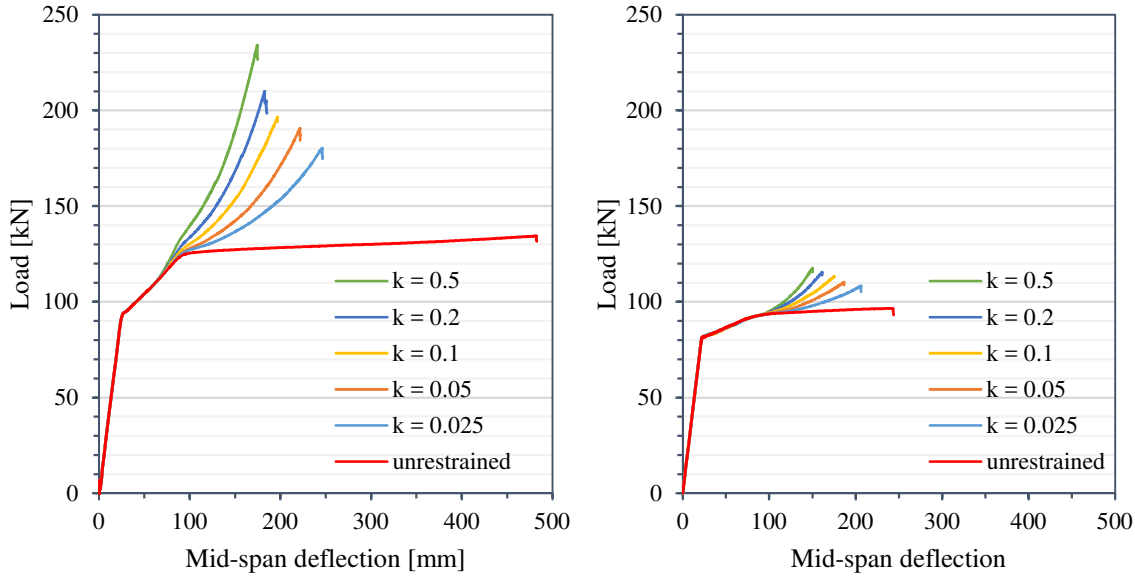

Figure 6: Load-deflection curves of precast HC slabs in TMA: a) HC150 (6 m span); b) HC200 (8 m span).

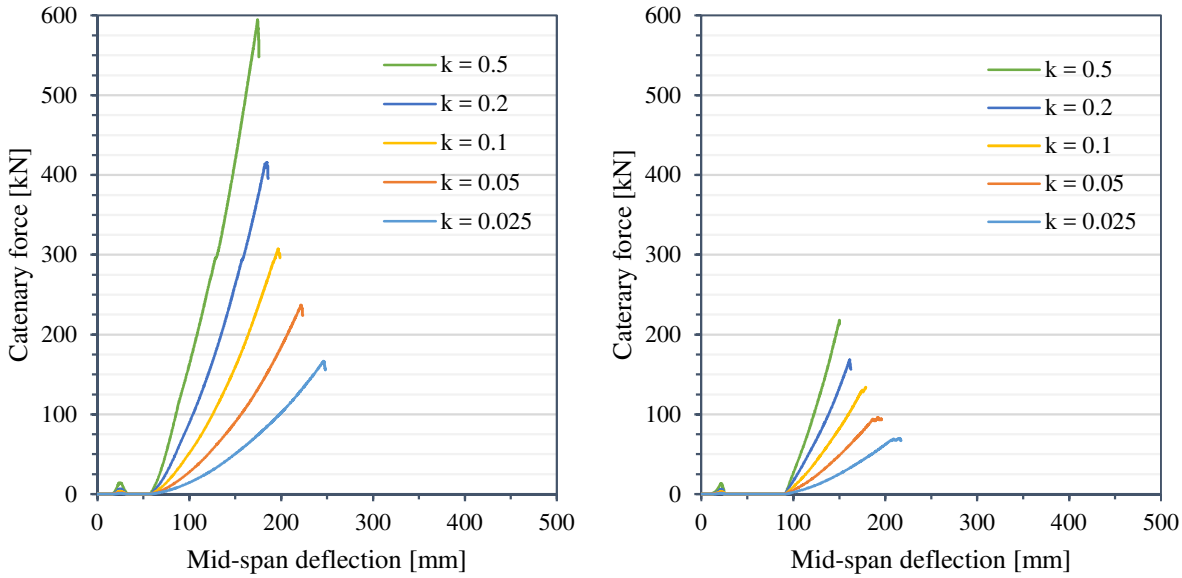

Figure 7: Catenary action in function of deflection: a) HC150 (6 m span); b) HC200 (8 m span).

In all simulations, the capacity reached a peak value in the TMA phase. Concurrent with this peak value, a flexural failure was observed, in which one or more of the prestressing strands reached the ultimate strain ε_u. To visualize the crack patterns, the concrete and steel plastic strains in the deformed geometry of a HC 150 section in TMA (k = 0.1) are visualized in Figure 8.a and b. Note that the numerical model does not track crack growth explicitly. Rather, the development of cracks can be indicated by areas of high plastic strains. Between the load points, various cracks are visible at the bottom edge. The largest cracks on the bottom surface are observed in the region where the loads are applied. From the visualization of the steel strains in Figure 8.b, it is clear that the strand failure also occurs at this location. Overall, the cracking patterns are very similar to those observed in experimental tests on regular reinforced concrete slabs in TMA (Gouverneur, 2014). Lastly, Figure 8.c depicts the tensile stresses in the prestressing strands just before the slab reaches its ultimate TMA capacity. The figure shows that the steel stress exceeds the yield stress (i.e. 1674 MPa) in the entire region between the load points. The locations where the prestressing strands failed are also clearly indicated.

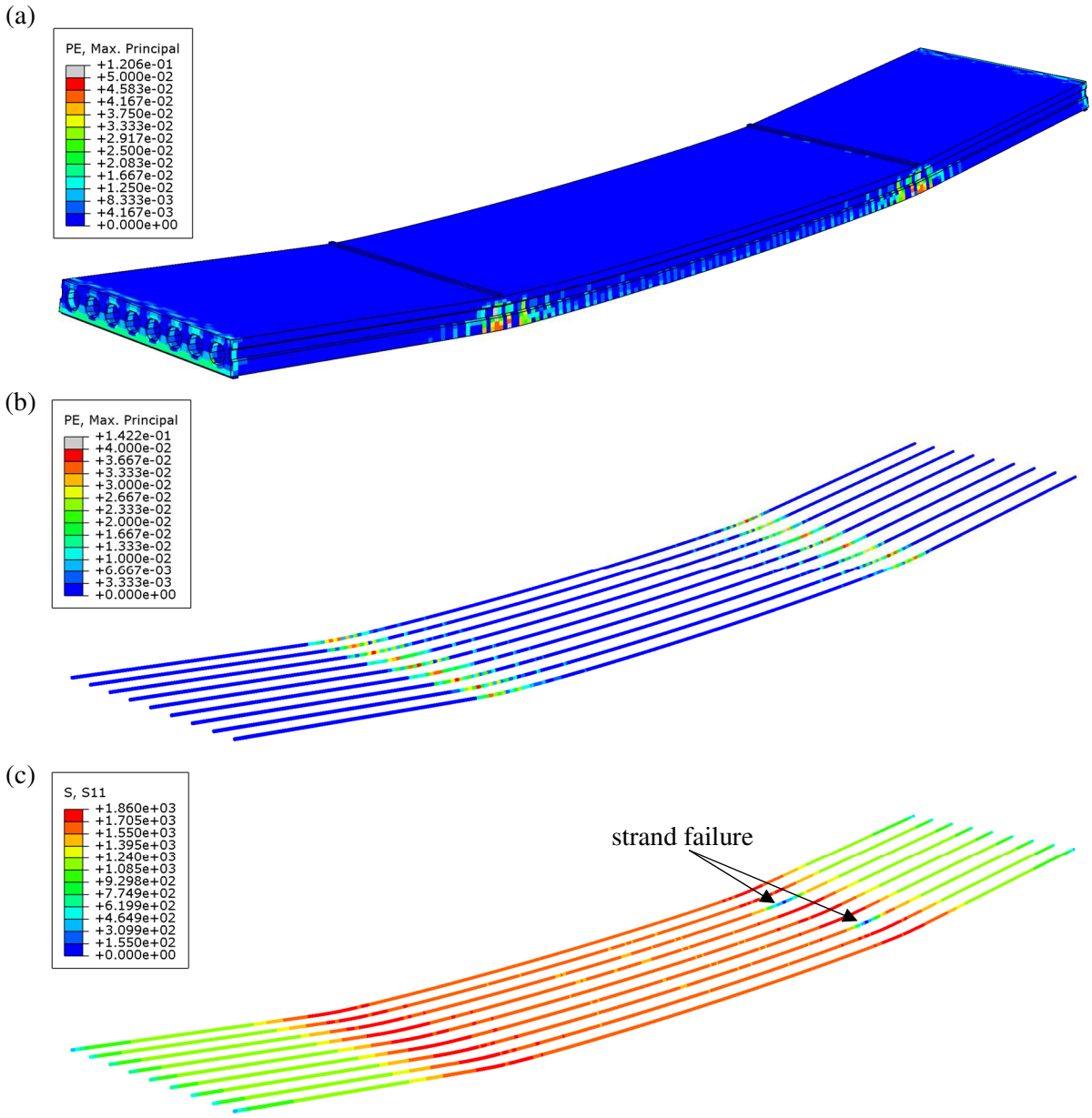

Figure 8: Precast slab HC150 in tensile membrane action (span length = 6 m, k = 0.1) at failure: a) concrete plastic strains; b) steel plastic strains; c) steel stresses (in MPa)

3.2. Influence of ultimate steel strain

Research towards the development of TMA in reinforced concrete members has revealed the large influence of the ultimate tensile strain of the reinforcement on the ultimate capacity (Botte, Caspeele, & Taerwe, 2015; Gouverneur, 2014). Increasing the reinforcement's ultimate strain has been shown to facilitate a more ductile behaviour of concrete members. Consequently, for larger ultimate reinforcement strains, significantly larger deflections can be obtained, and the TMA of the slab can further develop, which results in a higher ultimate load-carrying capacity of the slab (Droogné, 2019). In prestressing steel, the ultimate strain ε_u normally ranges from 0.05 to 0.07 (PCI, 1999). A minimum value of 0.02 is specified in *fib* Model Code 2010 (Comité Euro- International du Béton, 2010). Therefore, in the following, ultimate strain values ε_u ranging from 2% to 7% are considered.

The resulting load-deflection curves for the HC150 section with a span of 7.5 m are shown in Figure 9. In the figure, a relative horizontal restraint stiffness k = 0.1 was considered. The point at which the ultimate capacity is reached is indicated with a cross. From the graph, it is observed that the ultimate strain ε_u has a large influence on the ultimate capacity of HC slabs in TMA. Moreover, the ultimate mid-span deflection at failure, also increases considerably with increasing ultimate strain. Similar results were found for the HC200 sections.

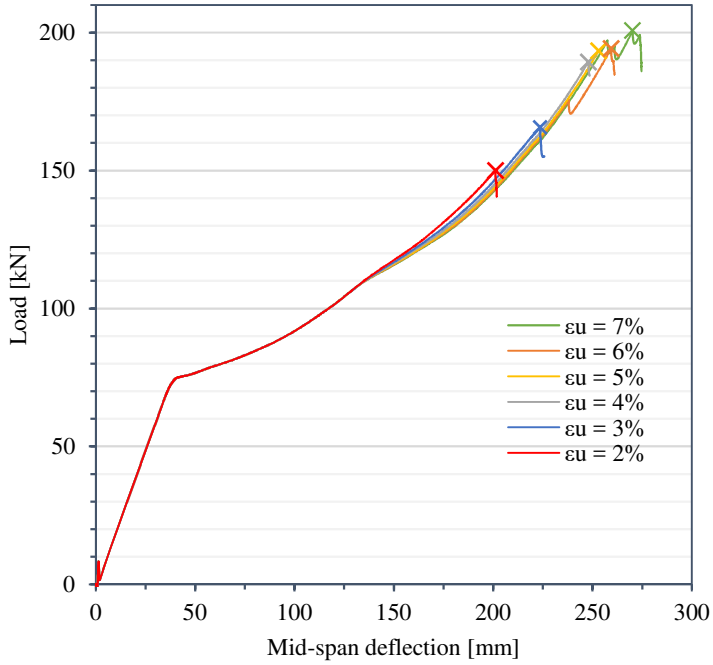

Figure 9: Influence of the ultimate strain of steel on the load-deflection diagrams of HC 150 slabs in TMA.

4. Conclusions and discussion

In the present study, the formation of tensile membrane action (TMA) was studied numerically. As a general conclusion, it was observed that the additional capacity that can be achieved through the activation of TMA is rather limited, especially when compared to the additional capacity that can be reached through compressive membrane action. From the results obtained through the numerical modelling of restrained hollow core slabs, several additional conclusions can be drawn.

- The cracking patterns observed during the large deformations that characterize the TMA phase were very similar to those observed in experimental tests on solid reinforced concrete slabs.
- The amount of axial restraint required to activate TMA is relatively small. In the studied HC150 slab, even a restraint stiffness equal to 2.5% the axial stiffness of the HC member resulted in an additional capacity of up to 30%.

- The reserve capacity which can be activated due to TMA strongly depends on the ultimate strain of the prestressing steel. More ductile prestressing steel results in higher ultimate capacities and larger deformation at failure.

Further research is needed to generalize the presented results for geometries with larger spans, as well as hollow core floor elements with other geometries and reinforcement configurations. Moreover, to complete the picture, the combined effect of compressive membrane action and tensile membrane action requires more in-depth investigation, to identify which of these phenomena leads to the highest reserve capacity. Lastly, the influence of a commonly applied second phase topping layer on the additional load bearing capacity needs further study.

Acknowledgements

The authors wish to thank the Research Foundation of Flanders (FWO) for the financial support on the research project "Performance-based analysis and design for enhancing the safety of prestressed concrete hollow-core slabs in case of fire and unforeseen events".

References

Botte, W., Caspeele, R., & Taerwe, L. (2015). Tensile membrane action in RC slabs: A parametric study. *Safety, Robustness and Condition Assessment of Structures*, 178–185. https://doi.org/10.2749/222137815815622861

Brotchie, J. F., & Holley, M. J. (1971). Membrane Action in Slabs. *ACI Symposium Publication*, *30*, 345–377. https://doi.org/10.14359/17503

CEN. (2004a). *EN 1992-1-1. Eurocode 2: Design of concrete structures - Part 1-1: General rules and rules for buildings*. Brussels.

CEN. (2004b). *EN 1992-1-2. Eurocode 2 – design of concrete structures. Part 1–2: general rules – structural fire design*. Brussels.

Comité Euro- International du Béton. (2010). *CEB-FIP Model Code 2010: design code*. Retrieved from http://repositorio.unan.edu.ni/2986/1/5624.pdf

Dassault Systemes. (2014). *Abaqus 6.14: Abaqus/CAE User's Guide*. Providence, USA.

Droogné, D. (2019). *Reliability-based design for robustness: evaluation of progressive collapse in concrete structures taking into account membrane action*. Ghent University.

Gouverneur, D. (2014). *Experimental and Numerical analysis of tensile membrane action in reinforced concrete slabs in the framework of strucural robustness, PhD thesis*. Ghent University.

Gouverneur, D., Caspeele, R., & Taerwe, L. (2013). Experimental investigation of the load-displacement behaviour under catenary action in a restrained reinforced concrete slab strip. *Engineering Structures*, *49*, 1007–1016. https://doi.org/10.1016/j.engstruct.2012.12.045

Guice, L. K., & Rhomberg, E. J. (1988). Membrane Action in Partially Restrained Slabs. *ACI Structural Journal*, *85*(4). https://doi.org/10.14359/2517

Muthu, K. U., Amarnath, K., Ibrahim, A., & Mattarneh, H. (2007). Load deflection behaviour of partially restrained slab strips. *Engineering Structures*, *29*(5), 663–674. https://doi.org/10.1016/j.engstruct.2006.05.017

PCI. (1999). *PCI Handbook Precast Prestressed Concrete*. Chicago: Precast/Prestressed Concrete Institute.

Thienpont, T., Caspeele, R., & De Corte, W. (2020). Additional load bearing capacity of prestressed hollow core slabs due to membrane action. *Proceedings of the Fib Symposium 2020*, 1683–1689. Shanghai.

Vecchio, F. J., & Tang, K. (1990). Membrane action in reinforced concrete slabs. *Canadian Journal of Civil Engineering*, *17*, 686–697.

Walraven, J. C., & Mercx, W. P. M. (1983). The bearing capacity of prestressed hollow core slabs. *Heron*, *28*(3).